

UNIVERSITÀ POLITECNICA DELLE MARCHE
Repository ISTITUZIONALE

Driver's Mental Workload Monitoring by Unobtrusive Textile Electrodes on the Wheel

This is the peer reviewd version of the followng article:

Original
Driver's Mental Workload Monitoring by Unobtrusive Textile Electrodes on the Wheel / Bomprezzi, L., Bruschi, V., Cecchi, S., Ciattaglia, G., Spinsante, S., Terenzi, A.. - (2026), pp. 102-107. (6th IEEE International Workshop on Metrology for Automotive, IEEE MetroAutomotive 2026 Brescia, IT 17 - 19 June 2026) [10.1109/MetroAutomotive69354.2026.11644659].

Availability:
This version is available at: 11566/365693 since: 2026-10-30T08:52:10Z

Publisher:
Institute of Electrical and Electronics Engineers Inc.

Published
DOI:10.1109/MetroAutomotive69354.2026.11644659

Terms of use:

The terms and conditions for the reuse of this version of the manuscript are specified in the publishing policy. The use of copyrighted works requires the consent of the rights' holder (author or publisher). Works made available under a Creative Commons license or a Publisher's custom-made license can be used according to the terms and conditions contained therein. See editor's website for further information and terms and conditions.
This item was downloaded from IRIS Università Politecnica delle Marche (https://iris.univpm.it). When citing, please refer to the published version.

Publisher copyright:

IEEE - Postprint/Author's Accepted Manuscript

©2026 IEEE. Personal use of this material is permitted. Permission from IEEE must be obtained for all other uses, in any current or future media, including reprinting/republishing this material for advertising or promotional purposes, creating new collective works, for resale or redistribution to servers or lists, or reuse of any copyrighted component of this work in other works. To access the final edited and published work see 10.1109/MetroAutomotive69354.2026.11644659

(Article begins on next page)

28 November 2026

Driver's Mental Workload Monitoring by Unobtrusive Textile Electrodes on the Wheel

Luca Bomprezzi
Dept. of Information Engineering
Università Politecnica delle Marche
Ancona, Italy
S1109924@studenti.univpm.it

Valeria Bruschi
Department of Information Engineering
Università Politecnica delle Marche
Ancona, Italy
v.bruschi@staff.univpm.it

Stefania Cecchi
Department of Information Engineering
Università Politecnica delle Marche
Ancona, Italy
s.cecchi@staff.univpm.it

Gianluca Ciattaglia
Department of Information Engineering
Università Politecnica delle Marche
Ancona, Italy
g.ciattaglia@staff.univpm.it

Susanna Spinsante
Department of Information Engineering
Università Politecnica delle Marche
Ancona, Italy
s.spinsante@staff.univpm.it

Alessandro Terenzi
Department of Information Engineering
Università Politecnica delle Marche
Ancona, Italy
a.terenzi@staff.univpm.it

***Abstract*—Road traffic accidents attributed to fatigue and drowsiness of drivers remain a major global safety concern, requiring the development of unobtrusive monitoring systems. This paper presents a comparative analysis of a novel contact-based sensing system designed to monitor driver mental workload using silver-based textile electrodes integrated into a steering wheel. Unlike traditional Ag/AgCl finger electrodes, which can interfere with the driving task, the proposed textile sensor offers an unobtrusive and long-term tolerable alternative. Experiments were conducted using a high-fidelity driving simulator with seven subjects to compare the textile system's performance against a reference unit (ProComp Infiniti). Due to motion artifacts inherent in manual steering, frequency-domain analysis of Skin Conductance (SC) signals was employed. Results demonstrate that the prototype textile-based system provides Power Spectral Density (PSD) distributions nearly identical to the reference system. Specifically, the $0.25\,\mathrm{Hz}$ to $0.4\,\mathrm{Hz}$ sub-band was identified as a stable and sensitive band for identifying stress induced by driving. These findings, though preliminary, confirm the viability of silver-based textile electrodes for real-world automotive driver monitoring applications.**

***Index Terms*—Textile electrodes, skin conductance, instrumented wheel, driver monitoring, driving simulator.**

I. Introduction

Today, the car is the most commonly used means of transport and consequently road traffic accidents have risen sharply, becoming the foremost cause of injury-related deaths and the eighth leading cause of mortality worldwide [1]. The National Highway Traffic Safety Administration in the U.S. estimated 633 deaths due to drowsy driving in 2023 [2]. In a 2023 report, the European Commission's Mobility and Transport division highlighted the dangerous interplay between driving and fatigue, which is estimated to contribute to between 10 % and 20 % of all collisions [3]. It is unfortunately not currently possible to determine with precision the number of accidents, injuries, and fatalities attributable to drowsy driving, as it is often unfeasible to conclusively establish whether drowsiness was the causal factor in a crash, particularly in cases resulting in fatalities. Dangers arising from drowsy driving persist even when the driver does not actually fall asleep. States of drowsiness reduce attentiveness to the surrounding environment and increase susceptibility to distraction, thereby slowing reaction times, impairing the ability to avoid roadway hazards, and ultimately degrading decision-making processes, which may in turn lead to risky behaviors behind the steering wheel [4].

To address this issue, smart systems equipped with multiple sensors have been proposed in recent years to monitor the driver's mental workload [5]. Based on the type of sensors used, they can be classified into two categories: contactless and contact systems [6]. In both cases, the underlying principle is that sensors should be installed to avoid interfering with the driver, thereby ensuring a pleasant driving experience. Contactless systems are based on sensors located inside the vehicle cabin and focused on the driver. Examples of contactless methods are cameras that analyse the driver's face [7], [8], or radar sensors that are capable of acquiring physiological parameters of the driver [9], [10]. Although these systems are advantageous in that they do not interfere with the driving task, they rely on complex hardware infrastructures to operate/collect data and may exhibit performance degradation when exposed to adverse environmental conditions, such as light variations, vibrations, and occlusions. Conversely, contact-based sensing methods can provide more accurate information about the driver, despite the challenge of installing such sensors in a manner that does not interfere with the driving experience.

In this context, the most effective approach to implementing contact-based sensing methods is the use of an instrumented steering wheel, onto which several sensors can be integrated [11]. An inertial measurement unit (IMU) is often integrated into the steering wheel to measure simple quantities like steering angle and angular velocity to extract driving

behaviour [12]. Force sensors are also integrated in the wheel since they provide the position of the driver's hands advising the driver of a possible danger situation [12], [13]. Electrocardiogram (ECG) and photoplethysmography (PPG) sensors can be integrated in a smart wheel, and these physiological signals are capable of identifying the onset of drowsiness with high accuracy, often before any observable behavioral manifestations appear [14]. Galvanic Skin Response (GSR), also known as Electro Dermal Activity (EDA), is an additional physiological parameter that can be acquired through the integration of dedicated electrodes in the steering wheel [15]. It is well established that variations in the skin's electrical properties under conditions of emotional arousal or mental workload can be leveraged for the detection of induced-stress states [16]. Moreover, unlike ECG and PPG, determining the driver's hand position and measuring GSR can be achieved using low-cost sensors that are easy to integrate.

Focusing on GSR, traditional time-domain analysis of the signal amplitude, usually applied in experiments involving auditory or visual stimuli, may not be able to detect the small changes arising in response to mental or cognitive workload when executing a task [17], especially in noisy acquisitions such as those performed on drivers, because of motion artifacts [18]. In fact, hands' movements required to maneuver the vehicle, like through tight traffic, add noise onto the collected signals by compromising the electrode-to-skin contact stability. This has considerable adverse consequences, especially in cases in which the Skin Conductance (SC) measure of EDA is acquired, which typically takes small values. Back in 2008, Shimomura et al. [19] found that conventional figures, specifically the rate of Skin Conductance Responses (SCRs) over time and their amplitude, failed to demonstrate a significant correlation with task difficulty. On the other hand, frequency-domain analysis could detect small differences originated by cognitive tasks. The frequency bandwidth considered in their study was $0.03\,\mathrm{Hz}$ to $0.5\,\mathrm{Hz}$. In [20], an auditory-based dual task scenario is investigated to understand drivers' behaviour, and a single bandwidth from $0.02\,\mathrm{Hz}$ to $0.2\,\mathrm{Hz}$ is considered. The analysis of the literature shows that, when processing SC signals, the choice of the number and width of the relevant frequency sub-bands depends on the type of stimulus administered to the subject. Posada-Quintero et al. in [21] and [22] defined the $0.045\,\mathrm{Hz}$ to $0.25\,\mathrm{Hz}$ range as the most sensitive one for sympathetic activation. The latter, which may be assumed as a gold band for resting and cognitive stress evaluation from SC signals analysis, is one of several sub-bands considered in this work to compare the SC acquisitions performed by means of prototype silver-based textile electrodes, and a reference acquisition system, the ProComp Infiniti one [23].

This paper presents the comparative analysis of the SC acquisitions from subjects engaged in the same simulated driving session, by means of a couple of silver-based textile electrodes and a reference acquisition system for bio-signals, used at the same time. The aim of the work is to compare the performance of the textile electrodes to the reference system based on the frequency-domain analysis of the corresponding signals, in supporting the detection of drivers' stress conditions, due to the mental workload generated by the test [24]. If the stress-related information within the SC signals is preserved, the silver-based textile electrodes could replace classical Ag/AgCl electrodes and be more comfortably applied on the wheel and used to monitor drivers in real settings.

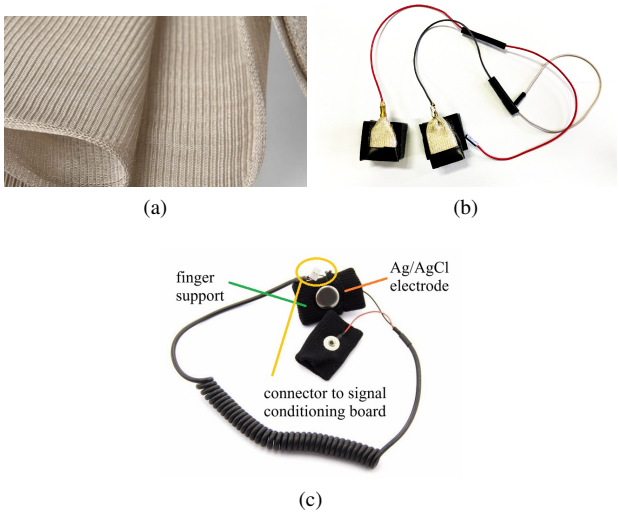

(a) (b) (c)

Fig. 1. (a) Silver-based fabric used to implement the textile electrodes for the unobtrusive SC sensor (from [25]), (b) preliminary design of the textile electrodes, and (c) the commercial Grove-GSR Sensor v1.2 electrodes and finger supports.

The paper is organized as follows: the silver-based textile sensor design and the hardware components selected to manage the sensor are presented in Section II, while Section III describes the experimental setup. Section IV reports the signal processing procedure applied to the acquired signals, while Section V describes the way experiments involving volunteers were performed. Section VI reports and discusses the obtained results, and Section VII summarizes the main conclusions of the work.

II. Silver-based textile sensor design

The unobtrusive sensor for driver's monitoring exploits textile electrodes made by a 99% Ag-based fabric provided by Soliani EMC [25] and shown in Fig. 1(a). Silver-based fabrics for creating electrodes for EDA acquisition have gained traction due to the unique properties of silver, such as its conductivity and antibacterial effects. In fact, silver is one of the best conductors of electricity (featuring a resistivity $\rho_{Ag} = 0.016\,\Omega\,\mathrm{mm}^2\,\mathrm{m}^{-1}$ at $20\,^{\circ}\mathrm{C}$, lower than copper and aluminum), less affected by oxidation than other conductive materials, making it suitable for electrodes. Moreover, silver fabrics can reduce skin irritation and infection risks, improving tolerability in long-term use applications [26].

The preliminary design of the textile electrodes is shown in Fig. 1(b): a finger-type modality was initially chosen, to have a direct comparison with the Grove-GSR Sensor v1.2 [27] available in the market as an Arduino UNO compatible sensor, equipped with typical Ag/AgCl electrodes settled onto

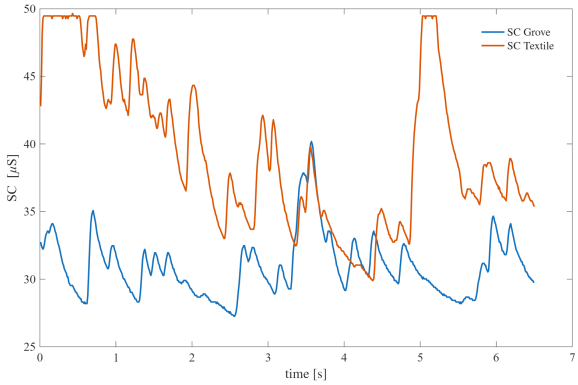

Fig. 2. Sample raw SC acquisitions from the same subject, using the silver-based textile electrodes (red curve) and the GSR sensor electrodes (blue curve).

stretch fabric supports for fingers, as shown in Fig. 1(c). The Grove-GSR Sensor typically includes a signal conditioning circuit based on the Texas Instruments LM324 configured as a non-inverting amplifier, to amplify and process the signals from the skin electrodes, and a low-pass filter to reduce high-frequency noise. The same conditioning circuit was used by replacing the original Grove-GSR Sensor electrodes with the silver fabric ones, and preliminary tests were executed on ten subjects, to compare the number of SCRs found by acquiring the SC with the two sensors, at the same time, under relaxed conditions. These initial tests showed that the sensor made with silver fabric electrodes consistently overestimated the number of SCRs with respect to the Ag/AgCl electrodes (in seven tests out of ten) so, in the following experiments, a frequency-domain processing of the signals was chosen. Signals acquired by the two systems exhibit differences in the absolute values of the skin conductance. A preliminary analysis on them showed an RMSE ranging from quite a low value of 2.9 µS to over 65 µS, while their time evolution appeared similar. An example of the raw SC acquisitions performed on the same subject from the different electrode pairs is shown in Fig. 2. For these reasons, the following considerations will focus on the percent Power Spectral Density (PSD) distribution over different sub-bands of interest.

III. Experimental Setup

The experimental setup, illustrated in Fig. 3, leverages a high-fidelity driving simulator. The hardware architecture comprises a Logitech G29 steering system and pedal set interfaced with a Dell G5 laptop. Visual feedback is provided via a large-format display positioned forward of the participant, who occupies a standard vehicle seat. Simulations are executed using the Assetto Corsa software (by Kunos Simulazioni), featuring a Lotus Evora car model. The experimental trials were conducted on a digital reconstruction of the Silverstone Circuit, characterized by a total length of 1.7 km. A detailed view of the instrumented steering wheel is given in Fig. 4, where it is possible to see one of the silver-based textile electrodes (2 cm × 38 cm) on the left side

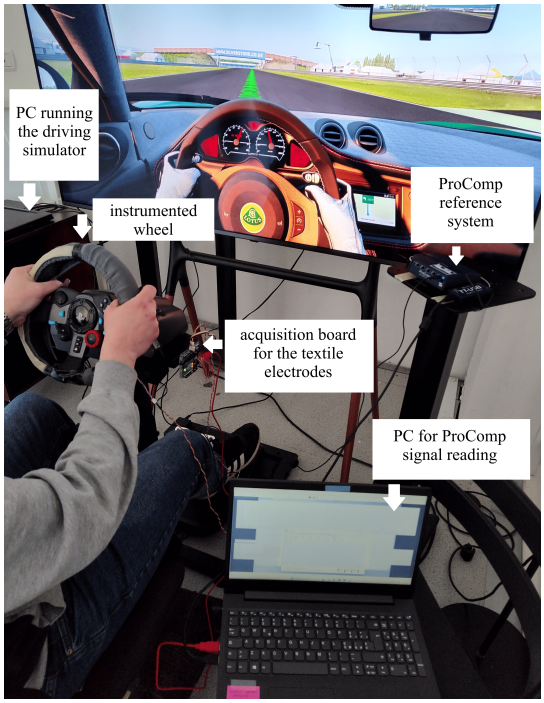

Fig. 3. Test setup and the main components.

of the wheel; the second electrode is located in the same position, but on the rear side of the wheel. The electrodes pair is wired to the same signal-conditioning circuit used for the Grove-GSR Sensor v1.2, implementing a resistive voltage divider and providing pre-amplification by an LM324 operational amplifier. One of the analog input pins available on an Arduino UNO board samples the voltage at a frequency $f_s = 100$ Hz and the corresponding digital values are saved on a log file for offline processing.

The reference physiological data acquisition is performed via the ProComp Infiniti system, a multi-channel digital acquisition (DAQ) unit [23]. The hardware architecture features five interchangeable input channels: the primary two channels support high-frequency signals, including Electroencephalography (EEG), Electrocardiography (ECG), and Heart Rate/Blood Volume Pulse (HR/BVP) at a sampling rate of 2048 Hz. The remaining three channels are dedicated to low-frequency modalities, such as respiration, temperature, and skin conductance, sampled at 256 Hz. For SC measurement, a Flex/Pro sensor with Ag/AgCl finger electrodes is employed, providing an input from 0 µS to 30 µS, with a calibrated accuracy of ±5% (±0.2 µS). The physical layer comprises a TT-USB interface unit and a fiber-optic link to ensure galvanic isolation, powered by four AA alkaline batteries. Data are encoded and transmitted via fiber optics to the TT-USB unit interfaced with the host PC. Post-acquisition processing and data exportation are managed through the BioGraph Infiniti software suite.

IV. Signal Processing

As mentioned in the Introduction section, in noisy acquisition conditions, the time-domain analysis of SC



Fig. 4. Driving simulator wheel with the silver-based textile electrode installed on the left half of the wheel.

signals amplitude may not be able to capture the variations originated by mental workload due to task execution. In the tests considered in this work, despite the simulated driving sessions, motion artifacts affect the acquired signals, because each subject has to physically interact with the instrumented steering wheel, by maneuvering it to perform the requested track. As such, frequency-domain processing of SC signals is applied. The dynamic and messy nature of driving combines cognitive workload, emotional stress (e.g., near-misses, traffic), and physical engagement, that cause the upper limit of the sympathetic frequency band to shift upward. The increased autonomic activity required to coordinate micro-movements can stretch the active sympathetic band up to $0.35\,\text{Hz}$ during highly erratic or high-speed driving simulations [28]. For this reason, the total bandwidth of interest in this study ranges from $0\,\text{Hz}$ to $1\,\text{Hz}$, and the sub-bands considered to compute the PSD distribution are: $0\,\text{Hz}$ to $0.045\,\text{Hz}$ (named B_1), $0.045\,\text{Hz}$ to $0.25\,\text{Hz}$ (named B_2), $0.25\,\text{Hz}$ to $0.4\,\text{Hz}$ (named B_3), and finally $0.4\,\text{Hz}$ to $1\,\text{Hz}$ (named B_4). While $0.5\,\text{Hz}$ is the absolute physiological limit of sweat gland response that originates variations in SC, the $0.25\,\text{Hz}$ cutoff is more robust for drivers, because steering maneuvers often introduce mechanical noise in the electrodes [21].

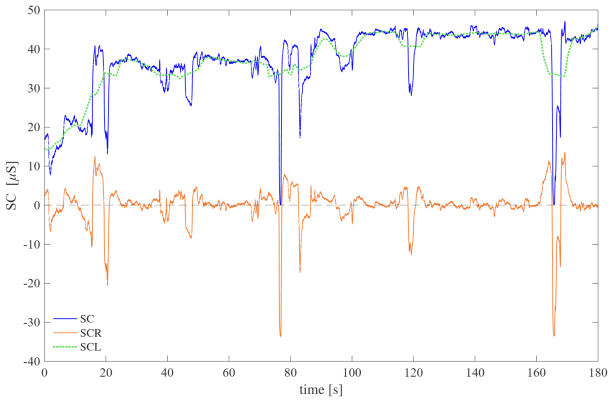

Fig. 5. Sample SC signal with its SCL and SCR components in the time domain.

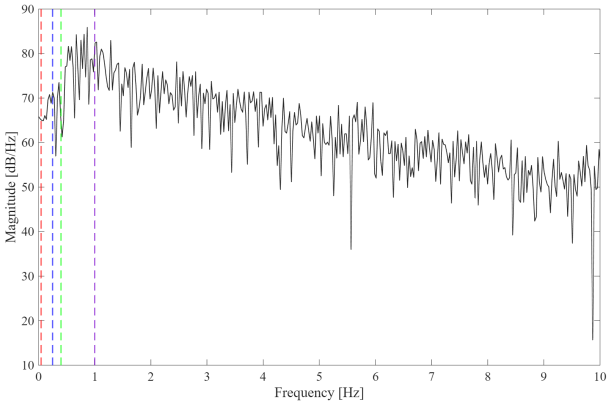

Fig. 6. Sample SCR signal spectrum and frequency sub-bands of interest.

Regarding the acquisitions performed by means of the silver-based textile electrodes, the collected physical quantity is actually a voltage, which is related to the human skin resistance by the equation (1) [27]:

$$R = \big((1024 + 2 \cdot v) \cdot 10^4\big)/(\alpha - v) \tag{1}$$

where R denotes the human skin resistance (given in Ω), v indicates the digital value output on the serial port by the acquisition board and corresponding to the detected voltage, while α is a tunable calibration parameter to provide the proper dynamic range for the acquisition. Based on preliminary tests, such parameter was set to 775 for all the acquisitions. The value 10^4 (given in Ω) denotes the fixed voltage divider resistor included in the signal conditioning circuit that provides pre-amplification [27]. As the acquisition board used in experiments features a $10\,\text{bit}$-resolution Analog-to-Digital Converter (ADC), 1024 gives the amount of Least Significant Bits (LSBs) available in the quantizer. A sampling frequency of $100\,\text{Hz}$ has been used. Once the human resistance value R is available, the SC value s is obtained as (2):

$$s = 10^6 \cdot 1/R \tag{2}$$

which is expressed in μS, as typically done in the literature. Each time series of SC values collected from a subject and obtained as described above, undergoes a filtering process by means of a sliding median filter ($4\,\text{s}$-long) designed to extract the so-called Skin Conductance Level (SCL) that accounts for the slow-time variation of the signal, which is not representative of the subject's reaction to the administered stimuli [29]. Such a signal is subtracted from the original one, to obtain the so-called phasic component (de-trended SC), or Skin Conductance Response (SCR) signal. Figure 5 shows a sample SC signal acquired from one of the test subjects, with its SCL and SCR components, obtained by the above-described steps. A few decreasing spikes can be spotted on the complete SC signal, typically due to motion artifacts affecting the acquisition in the time-domain. Later on, the SCR signal is processed by a Fast Fourier Transform (FFT) and the percent PSD within each frequency sub-band of interest

TABLE I

PERCENT PSD OVER FREQUENCY SUB-BANDS OF SC SIGNALS COLLECTED BY TEXTILE ELECTRODES AND ARDUINO (Σ_1), BY AG/AGCL ELECTRODES AND PROCOMP (Σ_2), AND THEIR DIFFERENCE (Δ_{2-1}) IN PERCENT POINTS (PP)

Subject	%PSD											
	B_1 0 Hz to 0.045 Hz			B_2 0.045 Hz to 0.25 Hz			B_3 0.25 Hz to 0.4 Hz			B_4 0.4 Hz to 1 Hz		
	Σ_1	Σ_2	Δ_{2-1}	Σ_1	Σ_2	Δ_{2-1}	Σ_1	Σ_2	Δ_{2-1}	Σ_1	Σ_2	Δ_{2-1}
S1	5.6	7.3	1.7	31.0	30.5	-0.5	17.8	15.8	-2	45.5	46.4	0.9
S2	5.1	5.4	0.3	29.7	26	-3.7	17.2	15.9	-1.3	48.0	52.6	4.6
S3	5.0	6.9	1.9	26.5	30.1	3.6	17.0	16.6	-0.4	51.4	46.3	-5.1
S4	5.0	5.6	0.6	24.4	25.2	0.8	16.8	16.5	-0.3	53.7	52.7	-1
S5	4.4	6.2	1.8	25.4	28.1	2.7	16.5	17.5	1	53.7	48.2	-5.5
S6	5.5	5.7	0.2	27.2	26.4	-0.8	16.4	15.4	-1	50.8	52.5	1.7
S7	4.7	5.6	0.9	24.5	25.6	1.1	15.7	16.1	0.4	55.1	52.6	-2.5

is computed by integration. Figure 6 shows the spectrum of the same signal given in Fig. 5, with the vertical dotted lines used to distinguish the four sub-bands of interest to analyze the signal.

Regarding the signals acquired at a sampling frequency of 256 Hz by the reference system, they are already output as SC values, expressed in µS, so they are filtered by the sliding median filter first, then the SCR is obtained, which is Fourier-transformed and integrated, to obtain the percent PSD values within each sub-band.

V. EXPERIMENTS

Experimental tests at the driving simulator involved a group of seven participants (5 males, 2 females) of age ranging from 17 to 49 years, all in a good state of health. Each subject was asked to sit on the driving simulator seat and take a first free driving test, to become familiar with the simulator and the driving controls. Then, before starting the 180 s-long acquisition, each participant was instrumented with the ProComp SC sensor electrodes on their index and middle fingers of the right hand. Once the subject was ready, the test started and the acquisition of the data values from the textile electrodes and from the ProComp was coordinated by an operator, ensuring the correct storage of the values on data files saved on the laptop controlling both the ProComp (via the BioGraph Infiniti software interface), and the Arduino UNO board (via the CoolTerm serial port monitoring software). Stress was induced by requiring each participant to complete an error-free lap within 180 s. By resetting the simulator at the start of each new trial, every participant was exposed to identical testing conditions; the ground-truth, stress-related SC signal was provided by the ProComp and used to test the Arduino-based system.

VI. RESULTS AND DISCUSSION

This section provides first a subject-by-subject discussion of how the percent PSD is distributed across the four sub-bands for each acquisition setup (textile electrodes and Arduino board versus Ag/AgCl electrodes and ProComp DAQ), and then how the two setups compare for the same subject, based on the results reported in Tab. I.

For subject S1, the two systems provide nearly identical distribution of the PSD over the sub-bands; ProComp shifts a little energy from B_3 to B_1 and slightly increases B_4. In the case of subject S2, ProComp concentrates relatively more power in the highest band B_4, mainly at the expense of the mid bands B_2 and B_3. Compared to textile-based system, ProComp shifts energy from B_4 to B_2 (and B_1), flattening the high-frequency dominance, in the test regarding subject S3. For subject S4, essentially the same pattern is exhibited across devices: differences are small and balanced. On the contrary, subject S5 exhibits the largest discrepancy between devices: ProComp redistributes a meaningful portion of the PSD from B_4 into $B_{1\text{-}3}$, especially B_2. For subject S6, ProComp strengthens the high-frequency band B_4 a bit, shaving from mid bands, and finally, in subject S7, ProComp mildly reduces B_4 and boosts lower bands.

On a cross-subjects basis, for every subject and both devices, the sub-bands ranking is consistent: B_4 dominates, followed by B_2, then B_3, with B_1 lowest. Sub-band B_1 is systematically higher with ProComp, up to 1.9 percent points (pp) in S3. Sub-band B_4 can perform either way, with largest differences (more than 5 pp) in S3 and S5, while sub-band B_2 often trades off inversely with B_4: when ProComp raises B_4, B_2 tends to drop (e.g., S2, S6), and vice versa (e.g., S3, S5). The average percent point difference of PSD over the four sub-bands is 1.06 pp for B_1, 0.46 pp for B_2, -0.51 pp for B_3, and -0.98 for B_4, confirming the acceptability of the presented system accuracy. Most interesting, for the aim of our study, it appears the behavior of the acquisitions performed by textile electrodes in B_3, namely the frequency sub-band considered to identify driving-induced stress: the percent PSD falling within this sub-band shows small changes ($\pm$ 1–2 pp) across the subjects, also remaining a stable mid-band across devices.

VII. CONCLUSION

This paper presented an attempt to use silver-based textile electrodes integrated into a steering wheel as a viable, unobtrusive alternative to traditional Ag/AgCl finger electrodes for monitoring Skin Conductance. Frequency-domain analysis of the collected signals, specifically looking at PSD, proved effective at capturing small changes related to cognitive workload. The prototype textile-based system provided PSD distributions nearly identical to the reference system. While

the latter occasionally showed higher sensitivity in the lowest frequency band, the textile electrodes maintained consistent performance in the critical workload-related bands, especially the $0.25\,\mathrm{Hz}$ to $0.4\,\mathrm{Hz}$ one, identified as the most stable and sensitive band for identifying stress induced by mental workload. Future works will extend the test population to confirm the preliminary results herein presented, possibly testing in real driving scenarios, and also address the possibility to use the same electrodes to locate the driver's hands position on the wheel.

ACKNOWLEDGMENT

The contribution of the Italian Ministry of Industry and Made in Italy, Fondo Crescita Sostenibile – Accordi di Innovazione, with project "Epignosis", CUP B39J23002460005, Project n. F/340008/04/X59 is acknowledged. The support of the company Soliani EMC S.r.l. (Italy) providing the silver-based fabric for prototyping the sensor electrodes is gratefully acknowledged.

REFERENCES

[1] S. M. Varnosfaderani, M. R. Shaikh, and M. Forouzanfar, "A Comprehensive Review of Unobtrusive Biosensing in Intelligent Vehicles: Sensors, Algorithms, and Integration Challenges," *Bioengineering*, vol. 12, no. 6, 2025. [Online]. Available: https://www.mdpi.com/2306-5354/12/6/669

[2] "Drowsy Driving - by National Highway Traffic Safety Administration," https://www.nhtsa.gov/risky-driving/drowsy-driving, accessed on: 2026-02-16.

[3] "European Commission's Mobility and Transport division Report," https://road-safety.transport.ec.europa.eu/european-road-safety-observatory/statistics-and-analysis-archive/fatigue, accessed on: 2026-02-16.

[4] E. Suni and A. Rehman, "Drowsy Driving," https://www.sleepfoundation.org/drowsy-driving, accessed on: 2025-03-26.

[5] V. Bruschi, S. Cecchi, A. Terenzi, D. Di Leo, G. Ciattaglia, and S. Spinsante, "Unobtrusive Driving Attitude Monitoring Through an Instrumented Steering Wheel," in *IEEE International Workshop on Metrology for Automotive (MetroAutomotive)*, 2025.

[6] M. S. Al-Quraishi, S. S. A. Ali, A.-Q. Muhammad, T. B. Tang, and S. Elferik, "Technologies for detecting and monitoring drivers' states: A systematic review," *Heliyon*, vol. 10, no. 20, p. e39592, 2024.

[7] A. Generosi, V. Bruschi, S. Cecchi, N. A. Dourou, R. Montanari, and M. Mengoni, "An Innovative System for Driver Monitoring and Vehicle Sound Interaction, year=2024," in *2024 IEEE International Workshop on Metrology for Automotive (MetroAutomotive)*, pp. 159–164.

[8] V. Bruschi, A. Generosi, N. Dourou, S. Spinsante, M. Mengoni, and S. Cecchi, "Vehicle Sound Interaction: A Preliminary Study on Driver's Experience Affected by Immersive Sound Reproduction," in *International Conference on Immersive and 3D Audio (I3DA 2025)*, 2025.

[9] G. Ciattaglia, S. Spinsante, and E. Gambi, "Slow-Time mmWave Radar Vibrometry for Drowsiness Detection," in *2021 IEEE International Workshop on Metrology for Automotive (MetroAutomotive)*, 2021, pp. 141–146.

[10] B. Li, W. Li, Y. He, W. Zhang, and H. Fu, "RadarNet: Noncontact ECG Signal Measurement Based on FMCW Radar," *IEEE Transactions on Instrumentation and Measurement*, vol. 73, pp. 1–9, 2024.

[11] P. Visconti, G. Rausa, C. Del-Valle-Soto, R. Velázquez, D. Cafagna, and R. De Fazio, "Innovative Driver Monitoring Systems and On-Board-Vehicle Devices in a Smart-Road Scenario Based on the Internet of Vehicle Paradigm: A Literature and Commercial Solutions Overview," *Sensors*, vol. 25, no. 2, 2025. [Online]. Available: https://www.mdpi.com/1424-8220/25/2/562

[12] M. Gobbi, F. Comolli, F. M. Ballo, and G. Mastinu, "Measurement data obtained by an instrumented steering wheel for driver model development," *Data in Brief*, vol. 30, p. 105485, 2020. [Online]. Available: https://www.sciencedirect.com/science/article/pii/S2352340920303796

[13] Y. Sahar, T. Elbaum, M. Wagner, O. Musicant, T. Hirsh, and S. Shoval, "Grip force on steering wheel as a measure of stress," *Frontiers in Psychology*, vol. 12, p. 617889, 2021.

[14] B. Babusiak, M. Smondrk, L. Trpis, T. Gajdosik, R. Madaj, and I. Gajdac, "Smart Steering Wheel Prototype for In-Vehicle Vital Sign Monitoring," *Sensors*, vol. 26, no. 2, 2026. [Online]. Available: https://www.mdpi.com/1424-8220/26/2/477

[15] A. Amidei, A. Poli, G. Iadarola, F. Tramarin, P. Pavan, S. Spinsante, and L. Rovati, "Driver drowsiness detection based on variation of skin conductance from wearable device," in *2022 IEEE International Workshop on Metrology for Automotive (MetroAutomotive)*. IEEE, 2022, pp. 94–98.

[16] B. Albert and T. Tullis, *Measuring the user experience: Collecting, analyzing, and presenting UX metrics*. Morgan Kaufmann, 2022.

[17] Williamson, James R. and Heaton, Kristin J. and Lammert, Adam and Finkelstein, Katherine and Sturim, Doug and Smalt, Christopher and Ciccarelli, Gregory and Quatieri, Thomas F., "Audio, Visual, and Electrodermal Arousal Signals as Predictors of Mental Fatigue Following Sustained Cognitive Work," in *2020 42nd Annual International Conference of the IEEE Engineering in Medicine and Biology Society (EMBC)*, 2020, pp. 832–836.

[18] Amin, Md. Rafiul and Alam, Samiul and Khazaei, Saman and Fekri Azgomi, Hamid and Faghih, Rose T., "Skin Conductance Response Artifact Reduction: Leveraging Accelerometer Noise Reference and Deep Breath Detection," *IEEE Access*, vol. 12, pp. 68 208–68 231, 2024.

[19] Y. Shimomura, T. Yoda, K. Sugiura, A. Horiguchi, K. Iwanaga, and T. Katsuura, "Use of Frequency Domain Analysis of Skin Conductance for Evaluation of Mental Workload," *Journal of PHYSIOLOGICAL ANTHROPOLOGY*, vol. 27, no. 4, pp. 173–177, 2008.

[20] J. Huang, Q. Zhang, T. Zhang, T. Wang, and D. Tao, "Assessment of Drivers' Mental Workload by Multimodal Measures during Auditory-Based Dual-Task Driving Scenarios," *Sensors*, vol. 24, no. 3, 2024. [Online]. Available: https://www.mdpi.com/1424-8220/24/3/1041

[21] H. F. Posada-Quintero, J. P. Florian, A. D. Orjuela-Cañón, T. Aljama-Corrales, and K. H. Chon, "Power Spectral Density Analysis of Electrodermal Activity for Sympathetic Function Assessment," *Annals of Biomedical Engineering*, vol. 44, no. 10, pp. 3124–3135, 2016. [Online]. Available: https://doi.org/10.1007/s10439-016-1606-6

[22] H. F. Posada-Quintero, N. Reljin, C. Mills, I. Mills, J. P. Florian, J. L. VanHeest, and K. H. Chon, "Time-varying analysis of electrodermal activity during exercise," *PLoS ONE*, vol. 13, no. 6, p. e0198328, 06 2018.

[23] Thought Technology Ltd., *ProComp Infiniti Hardware Manual*, https://thoughttechnology.com/, Thought Technology Ltd., Montreal, QC, Canada, 2017, sA7510 Rev. 7, accessed on: 2026-02-14.

[24] Li, Penghui and Li, Yibing and Yao, Yao and Wu, Changxu and Nie, Bingbing and Li, Shengbo Eben, "Sensitivity of Electrodermal Activity Features for Driver Arousal Measurement in Cognitive Load: The Application in Automated Driving Systems," *IEEE Transactions on Intelligent Transportation Systems*, vol. 23, no. 9, pp. 14 954–14 967, 2022.

[25] Soliani EMC, "Conductive and EMI Shielding Fabrics," https://www.solianiemc.com/p/tessuti-poliestere-nichel-emi-emc/, accessed on: 2026-02-15.

[26] S. Qureshi, G. M. Stojanović, M. Simić, V. Jeoti, N. Lashari, and F. Sher, "Silver Conductive Threads-Based Embroidered Electrodes on Textiles as Moisture Sensors for Fluid Detection in Biomedical Applications," *Materials*, vol. 14, no. 24, 2021. [Online]. Available: https://www.mdpi.com/1996-1944/14/24/7813

[27] "Seeed Studio, Grove GSR Sensor v. 1.2," https://wiki.seeedstudio.com/Grove-GSR_Sensor/, accessed on: 2026-02-14.

[28] H. F. Posada-Quintero and K. H. Chon, "Innovations in Electrodermal Activity Data Collection and Signal Processing: A Systematic Review," *Sensors*, vol. 20, no. 2, 2020. [Online]. Available: https://www.mdpi.com/1424-8220/20/2/479

[29] W. Boucsein, *Electrodermal activity*. Springer Science & Business Media, 2012.